

## Supporting Information

### **A Beam Path-based Method for Attenuation Correction of Confocal Micro-X-ray Fluorescence Imaging Data**

Peng Liu<sup>\*,a</sup>, Carol J. Ptacek<sup>a</sup>, David W. Blowes<sup>a</sup>, Y. Zou Finfrock<sup>b,c</sup>

*<sup>a</sup>Department of Earth and Environmental Sciences, University of Waterloo, 200 University Ave. W., Waterloo, ON, N2L 3G1, Canada*

*<sup>b</sup>CLS@APS sector 20, Argonne National Laboratory, 9700 S. Cass Avenue, Argonne, Illinois 60439, USA*

*<sup>c</sup>Science Division, Canadian Light Source Inc., 44 Innovation Boulevard, Saskatoon, Saskatchewan, S7N 2V3, Canada*

---

\* Corresponding author address: Department of Earth and Environmental Sciences, University of Waterloo, 200 University Ave. W., Waterloo, ON, N2L 3G1, Canada. Tel: +01 (519) 888 4567, ext. 37232  
E-mail: p26liu@uwaterloo.ca

Table S1. Elemental mass fraction of NIST SRM 1834 used for XRF correction.

Element	Content	Element	Content	Element	Content
H	1.00E-14	As	1.00E-14	Tb	1.00E-14
He	1.00E-14	Se	1.00E-14	Dy	1.00E-14
Li	4.60E-02*	Br	1.00E-14	Ho	1.00E-14
Be	1.00E-14	Kr	1.00E-14	Er	1.00E-14
B	6.20E-04*	Rb	2.00E-07 <sup>#</sup>	Tm	1.00E-14
C	1.00E-14	Sr	1.53E-03*	Yb	1.00E-14
N	1.00E-14	Y	5.00E-06 <sup>#</sup>	Lu	1.00E-14
O	4.80E-01*	Zr	4.70E-04*	Hf	1.07E-05 <sup>#</sup>
F	1.00E-14	Nb	1.00E-14	Ta	1.00E-14
Ne	1.00E-14	Mo	1.00E-06 <sup>#</sup>	W	1.00E-14
Na	1.40E-03*	Tc	1.00E-14	Re	1.00E-14
Mg	9.00E-04*	Ru	1.00E-14	Os	1.00E-14
Al	2.07E-01*	Rh	1.00E-14	Ir	1.00E-14
Si	2.09E-01*	Pd	1.00E-14	Pt	1.00E-14
P	1.35E-03*	Ag	1.00E-14	Au	1.00E-14
S	1.00E-14	Cd	1.00E-14	Hg	1.00E-14
Cl	1.00E-14	In	1.00E-14	Tl	1.00E-14
Ar	1.00E-14	Sn	1.00E-14	Pb	2.20E-06 <sup>#</sup>
K	4.20E-03*	Sb	1.00E-14	Bi	1.00E-14
Ca	9.50E-04*	Te	1.00E-14	Po	1.00E-14
Sc	1.00E-14	I	1.00E-14	At	1.00E-14
Ti	1.10E-02*	Xe	1.00E-14	Rn	1.00E-14
V	1.00E-14	Cs	2.00E-07 <sup>#</sup>	Fr	1.00E-14
Cr	2.00E-04*	Ba	6.20E-04*	Ra	1.00E-14
Mn	8.80E-04*	La	1.30E-07 <sup>#</sup>	Ac	1.00E-14
Fe	3.20E-03*	Ce	3.50E-07 <sup>#</sup>	Th	9.00E-08 <sup>#</sup>
Co	1.40E-07 <sup>#</sup>	Pr	1.00E-14	Pa	1.00E-14
Ni	5.00E-07 <sup>#</sup>	Nd	1.10E-07 <sup>#</sup>	U	4.00E-07 <sup>#</sup>
Cu	1.80E-05 <sup>#</sup>	Pm	1.00E-14	Np	1.00E-14
Zn	1.70E-05 <sup>#</sup>	Sm	1.00E-14	Pu	1.00E-14
Ga	1.00E-14	Eu	1.00E-14	Am	1.00E-14
Ge	1.00E-14	Gd	1.00E-14	Density	2.0 g cm <sup>-3</sup>

\* values from NIST SRM 1834 Certificate<sup>1</sup>

<sup>#</sup> values from Hollocher et al.<sup>2</sup>

Other values are entered as 10<sup>-14</sup> for correction purpose

Table S2. Elemental mass fraction of NIST SRM 611 used for XRF correction.

Element	Content	Element	Content	Element	Content
H	1.00E-14	As	3.03E-04 <sup>#</sup>	Tb	4.55E-04 <sup>#</sup>
He	1.00E-14	Se	1.15E-04 <sup>*</sup>	Dy	4.39E-04 <sup>#</sup>
Li	5.36E-04 <sup>#</sup>	Br	1.00E-14	Ho	4.60E-04 <sup>#</sup>
Be	4.81E-04 <sup>#</sup>	Kr	1.00E-14 <sup>#</sup>	Er	4.39E-04 <sup>#</sup>
B	2.26E-05 <sup>#</sup>	Rb	4.24E-04 <sup>#</sup>	Tm	4.23E-04 <sup>#</sup>
C	1.00E-14	Sr	4.92E-04 <sup>#</sup>	Yb	4.51E-04 <sup>#</sup>
N	1.00E-14	Y	4.70E-04 <sup>#</sup>	Lu	4.40E-04 <sup>#</sup>
O	5.65E-01 <sup>§</sup>	Zr	3.81E-04 <sup>#</sup>	Hf	3.13E-04 <sup>#</sup>
F	1.00E-14	Nb	2.49E-04 <sup>#</sup>	Ta	2.93E-04 <sup>#</sup>
Ne	1.00E-14	Mo	4.08E-04 <sup>#</sup>	W	1.00E-14
Na	1.02E-05 <sup>§</sup>	Tc	1.00E-14	Re	1.00E-14
Mg	4.88E-04 <sup>#</sup>	Ru	1.00E-14	Os	1.00E-14
Al	1.01E-02 <sup>§</sup>	Rh	1.00E-14	Ir	1.00E-14
Si	3.22E-01 <sup>§</sup>	Pd	1.00E-14	Pt	1.00E-14
P	3.05E-04 <sup>#</sup>	Ag	2.12E-04 <sup>#</sup>	Au	1.56E-05 <sup>#</sup>
S	1.00E-14	Cd	2.65E-04 <sup>#</sup>	Hg	1.00E-14
Cl	4.70E-04 <sup>#</sup>	In	4.61E-04 <sup>#</sup>	Tl	6.12E-05 <sup>#</sup>
Ar	1.00E-14	Sn	3.09E-04 <sup>#</sup>	Pb	3.89E-04 <sup>#</sup>
K	4.56E-04 <sup>#</sup>	Sb	3.40E-04 <sup>#</sup>	Bi	3.79E-04 <sup>#</sup>
Ca	8.14E-02 <sup>§</sup>	Te	1.00E-14	Po	1.00E-14
Sc	4.45E-04 <sup>#</sup>	I	1.00E-14	At	1.00E-14
Ti	4.37E-04 <sup>#</sup>	Xe	1.00E-14	Rn	1.00E-14
V	4.49E-04 <sup>#</sup>	Cs	3.20E-04 <sup>#</sup>	Fr	1.00E-14
Cr	3.81E-04 <sup>#</sup>	Ba	4.11E-04 <sup>#</sup>	Ra	1.00E-14
Mn	4.41E-04 <sup>#</sup>	La	4.33E-04 <sup>#</sup>	Ac	1.00E-14
Fe	4.61E-04 <sup>#</sup>	Ce	4.30E-04 <sup>#</sup>	Th	5.28E-04 <sup>#</sup>
Co	4.22E-04 <sup>#</sup>	Pr	4.63E-04 <sup>#</sup>	Pa	1.00E-14
Ni	4.46E-04 <sup>#</sup>	Nd	4.26E-04 <sup>#</sup>	U	5.13E-04 <sup>#</sup>
Cu	3.50E-04 <sup>#</sup>	Pm	1.00E-14	Np	1.00E-14
Zn	4.11E-04 <sup>#</sup>	Sm	4.49E-04 <sup>#</sup>	Pu	1.00E-14
Ga	4.37E-04 <sup>#</sup>	Eu	4.43E-04 <sup>#</sup>	Am	1.00E-14
Ge	3.91E-04 <sup>#</sup>	Gd	4.25E-04 <sup>#</sup>	Density	2.0 g cm <sup>-3</sup>

\* values from NIST SRM 611 Certificate<sup>3</sup>

# values from Pearce et al.<sup>4</sup>

§ values from Hinton<sup>5</sup>

Other values are entered as 10<sup>-14</sup> for correction purpose

Table S3. Elemental mass fraction of the fresh biochar particle used for XRF correction

Element	Content	Element	Content	Element	Content
H	5.00E-02 <sup>#</sup>	As	1.00E-14	Tb	1.00E-14
He	1.00E-14	Se	1.00E-14	Dy	1.00E-14
Li	1.00E-14	Br	1.00E-14	Ho	1.00E-14
Be	1.00E-14	Kr	1.00E-14	Er	1.00E-14
B	1.00E-14	Rb	1.00E-14	Tm	1.00E-14
C	7.02E-01*	Sr	1.80E-05*	Yb	1.00E-14
N	1.00E-02 <sup>#</sup>	Y	3.80E-07*	Lu	1.00E-14
O	1.51E-01 <sup>#</sup>	Zr	1.00E-10	Hf	1.00E-14
F	1.00E-14	Nb	1.00E-14	Ta	1.00E-14
Ne	1.00E-14	Mo	2.00E-07*	W	1.00E-14
Na	1.80E-05*	Tc	1.00E-14	Re	1.00E-14
Mg	2.10E-03*	Ru	1.00E-14	Os	1.00E-14
Al	1.60E-04*	Rh	1.00E-14	Ir	1.00E-14
Si	6.02E-02 <sup>‡</sup>	Pd	1.00E-14	Pt	1.00E-14
P	9.30E-04*	Ag	6.00E-08*	Au	1.00E-14
S	1.00E-03*	Cd	3.00E-08*	Hg	1.00E-14
Cl	1.50E-03 <sup>§</sup>	In	1.00E-14	Tl	1.00E-14
Ar	1.00E-14	Sn	7.00E-06*	Pb	4.70E-07*
K	9.30E-03*	Sb	1.00E-14	Bi	1.00E-14
Ca	9.20E-03*	Te	1.00E-14	Po	1.00E-14
Sc	1.00E-14	I	1.00E-10	At	1.00E-14
Ti	1.10E-05*	Xe	1.00E-14	Rn	1.00E-14
V	1.00E-14	Cs	1.00E-10	Fr	1.00E-14
Cr	3.40E-06*	Ba	2.20E-05*	Ra	1.00E-14
Mn	2.10E-04*	La	1.00E-14	Ac	1.00E-14
Fe	2.10E-03*	Ce	1.00E-14	Th	1.00E-14
Co	1.60E-07*	Pr	1.00E-14	Pa	1.00E-14
Ni	6.00E-07*	Nd	1.00E-14	U	8.00E-09*
Cu	7.20E-06*	Pm	1.00E-14	Np	1.00E-14
Zn	2.30E-05*	Sm	1.00E-14	Pu	1.00E-14
Ga	1.00E-14	Eu	1.00E-14	Am	1.00E-14
Ge	1.00E-14	Gd	1.00E-14	Density	0.3 g cm <sup>-3</sup>

\* values for the same batch from Liu et al.<sup>6</sup>, Liu et al.<sup>7</sup>, and Liu et al.<sup>8</sup>

The data obtained from the following references are all for switchgrass biochar pyrolyzed under similar conditions with the current study.

<sup>#</sup> values from Sadaka et al.<sup>9</sup>

<sup>§</sup> values from Cherney et al.<sup>10</sup>

<sup>‡</sup> values from El Bassam<sup>11</sup>

Other values are entered as 10<sup>-14</sup> for correction purpose

Table S4. Elemental mass fraction of the aged biochar particle used for XRF correction.

Element	Content	Element	Content	Element	Content
H	6.14E-02 <sup>#</sup>	As	4.40E-06*	Tb	1.00E-14
He	1.00E-14	Se	7.00E-07*	Dy	1.00E-14
Li	1.00E-10	Br	2.00E-05	Ho	1.00E-14
Be	1.00E-14	Kr	1.00E-14	Er	1.00E-14
B	1.00E-10	Rb	1.00E-10	Tm	1.00E-14
C	6.40E-01*	Sr	1.00E-10*	Yb	1.00E-14
N	1.00E-02 <sup>#</sup>	Y	1.00E-10*	Lu	1.00E-14
O	2.49E-01 <sup>#</sup>	Zr	1.00E-10	Hf	1.00E-10
F	1.00E-14	Nb	1.00E-14	Ta	1.00E-14
Ne	1.00E-14	Mo	1.00E-10*	W	1.00E-10
Na	1.60E-04*	Tc	1.00E-14	Re	1.00E-14
Mg	1.53E-03*	Ru	1.00E-14	Os	1.00E-14
Al	5.65E-03*	Rh	1.00E-14	Ir	1.00E-14
Si	2.00E-02 <sup>‡</sup>	Pd	1.00E-14	Pt	1.00E-10
P	9.30E-04*	Ag	1.00E-10	Au	1.00E-14
S	1.00E-03*	Cd	1.00E-10	Hg	2.00E-04*
Cl	1.50E-03 <sup>§</sup>	In	1.00E-14	Tl	1.00E-14
Ar	1.00E-14	Sn	1.00E-10*	Pb	1.00E-08
K	5.30E-03*	Sb	1.00E-14	Bi	1.00E-14
Ca	2.50E-03*	Te	1.00E-14	Po	1.00E-14
Sc	1.00E-10	I	1.00E-10	At	1.00E-14
Ti	1.88E-04*	Xe	1.00E-14	Rn	1.00E-14
V	1.00E-08	Cs	1.00E-10	Fr	1.00E-14
Cr	1.60E-04*	Ba	1.00E-10*	Ra	1.00E-14
Mn	4.60E-04*	La	1.00E-10	Ac	1.00E-14
Fe	6.00E-04*	Ce	1.00E-10	Th	1.00E-10
Co	1.30E-05*	Pr	1.00E-14	Pa	1.00E-14
Ni	1.60E-05*	Nd	1.00E-10	U	1.00E-10*
Cu	2.00E-04*	Pm	1.00E-14	Np	1.00E-14
Zn	1.20E-04*	Sm	1.00E-14	Pu	1.00E-14
Ga	1.00E-10	Eu	1.00E-14	Am	1.00E-14
Ge	1.00E-10	Gd	1.00E-14	Density	0.5 g cm <sup>-3</sup>

\* values for the same batch from Liu et al.<sup>6</sup> and Liu et al.<sup>7</sup>

The data obtained from the following references are all for switchgrass biochar pyrolyzed under similar conditions with the current study.

<sup>#</sup> values from Sadaka et al.<sup>9</sup>

<sup>§</sup> values from Cherney et al.<sup>10</sup>

<sup>‡</sup> values from El Bassam<sup>11</sup>

Other values are entered as 10<sup>-14</sup> for correction purpose

Table S5. Lower limit of detection (LLD,  $\mu\text{g g}^{-1}$ ) of selected elements from NIST 611.

Element	LLD
Ca	320( $\pm 30$ )
Ti	76( $\pm 6$ )
Fe	30( $\pm 3$ )
Co	29( $\pm 3$ )
Ni	25( $\pm 3$ )
Cu	19( $\pm 2$ )
Zn	18( $\pm 2$ )
Se	19( $\pm 2$ )
Rb	21( $\pm 2$ )
Sr	6.0( $\pm 0.6$ )
Pb	12( $\pm 1$ )
Bi	34( $\pm 3$ )
Th	36( $\pm 4$ )

Note: LLD was calculated using the method described by Smolek et al.<sup>12</sup>. The dwell time is 0.2 s. Spectra used for LLD calculation were collected from the surface of SRM 611. The high LLD of Ca was due to the high fraction of Ca in NIST SRM 611 (Table S2). The LLD depends on the resolution of the detector, the matrix of SRM 611, and the dwell time.

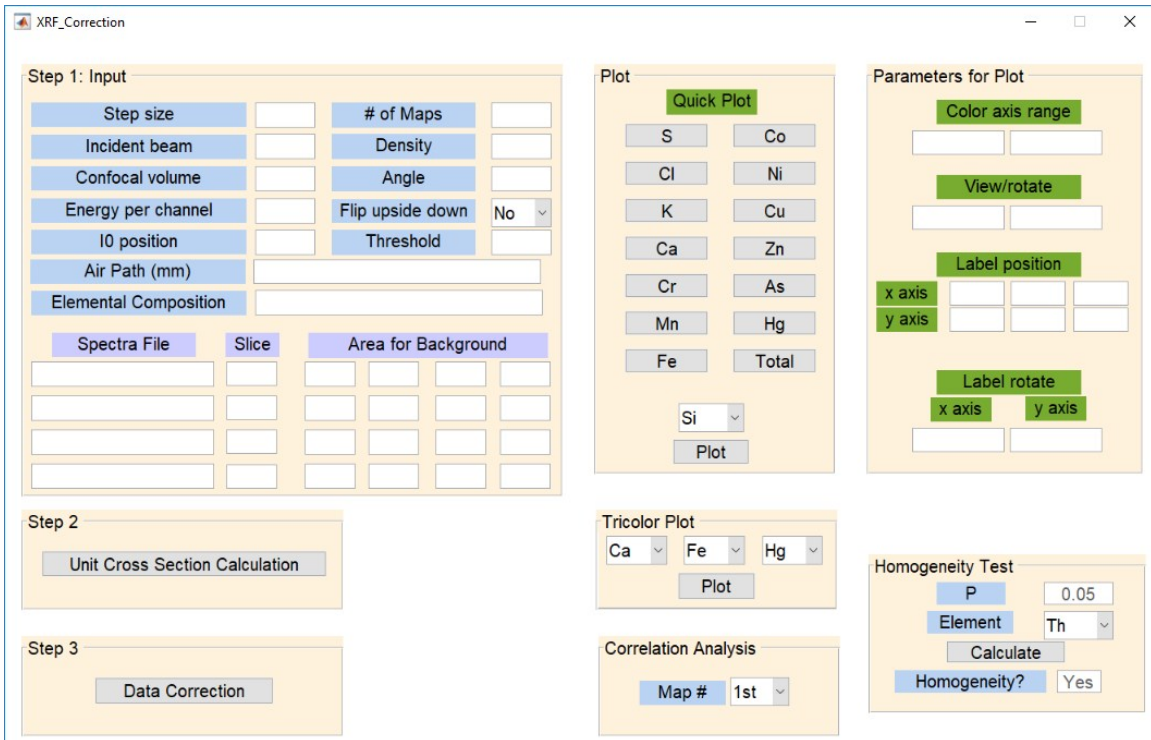


Figure S1. Screenshot of the correction method compiled in MATLAB®.

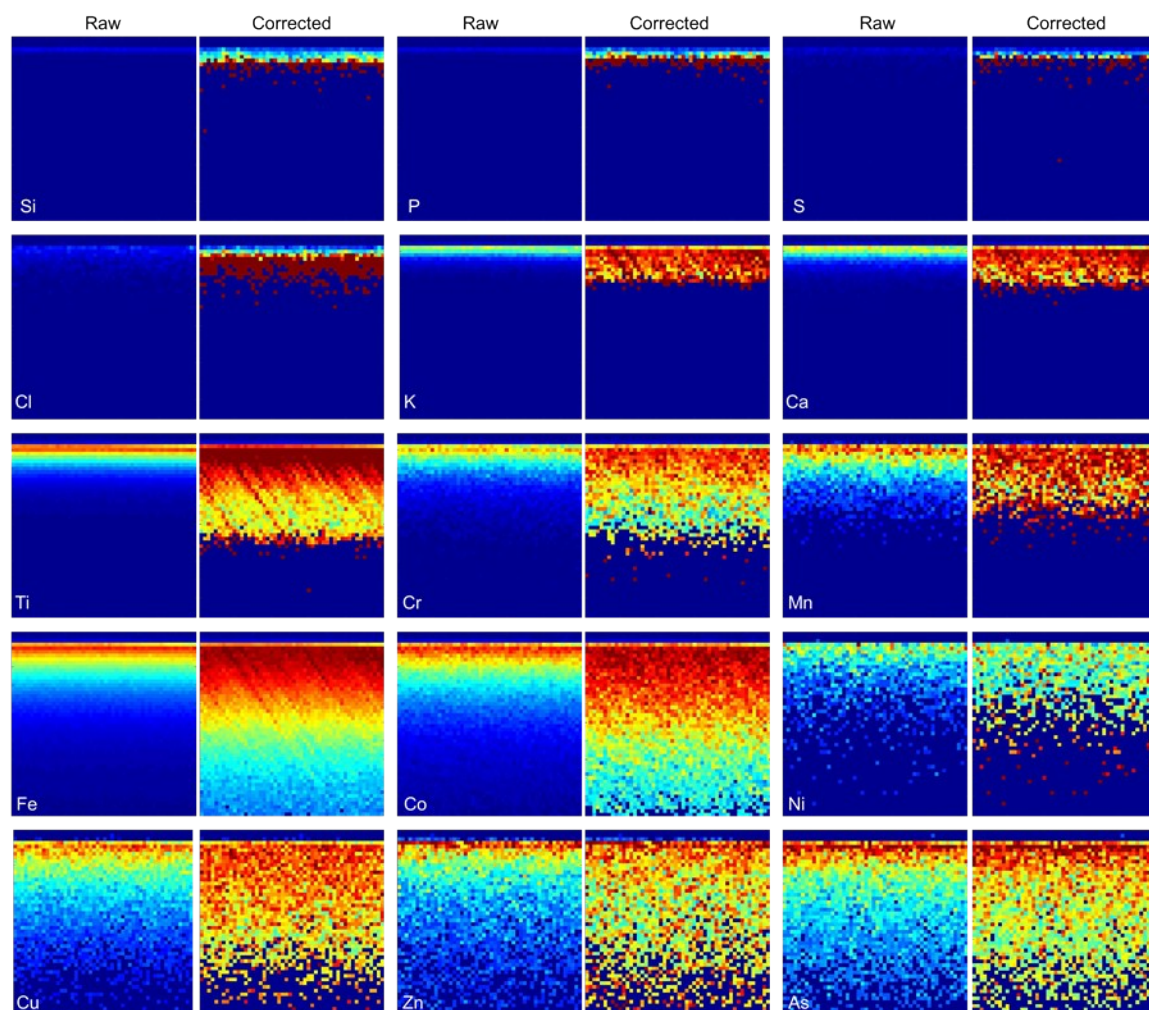


Figure S2. The raw and corrected data X-ray fluorescence of Si, P, S, Cl, K, Ca, Ti, Cr, Mn, Fe, Co, Ni, Cu, Zn, and As from SRM 1834 (simulated ore). The intensity distribution of dark matrix was assumed the same as As for correction purpose. The top of the imaging area is the surface of SRM 1834. The maps were plotted at the same intensity scale for the raw and corrected data for each element. The map size is 250×250  $\mu\text{m}$ .

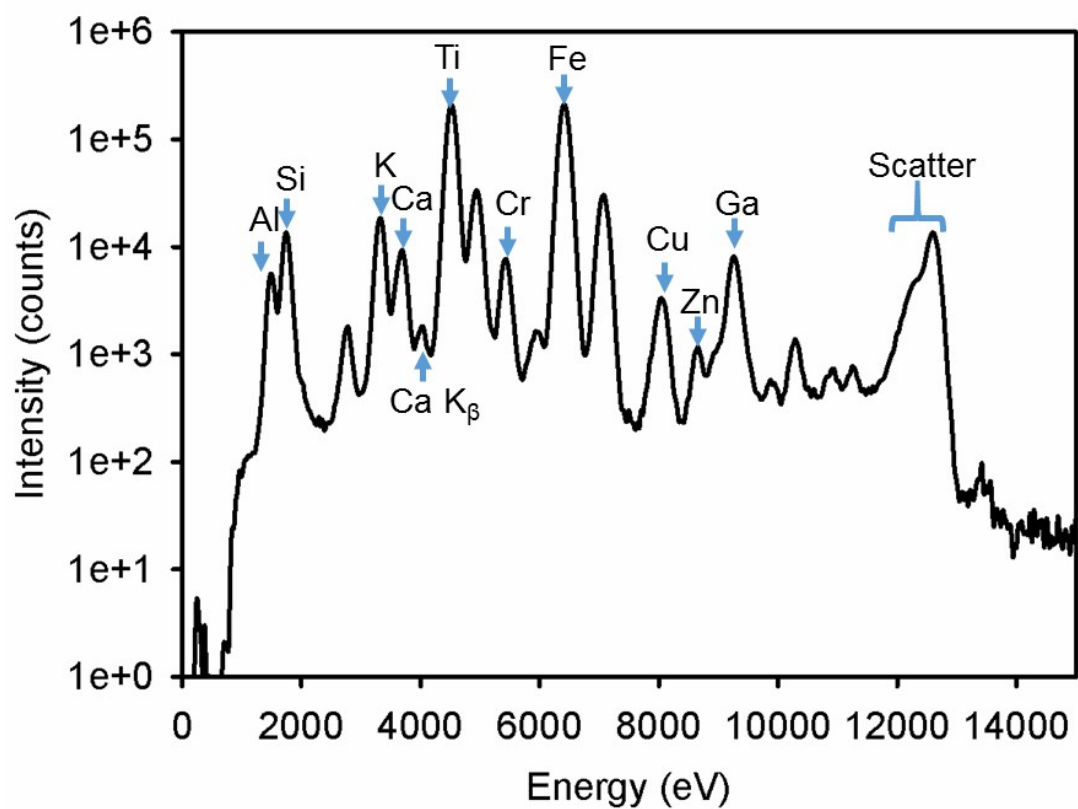


Figure S3. XRF spectrum collected from the surface area of SRM 1834 in Fig. S2. The peaks indicated by element name represent the  $K_{\alpha}$  line. The  $K_{\beta}$  line of Ca and scatter are also labeled. The incident energy was 12.6 keV.

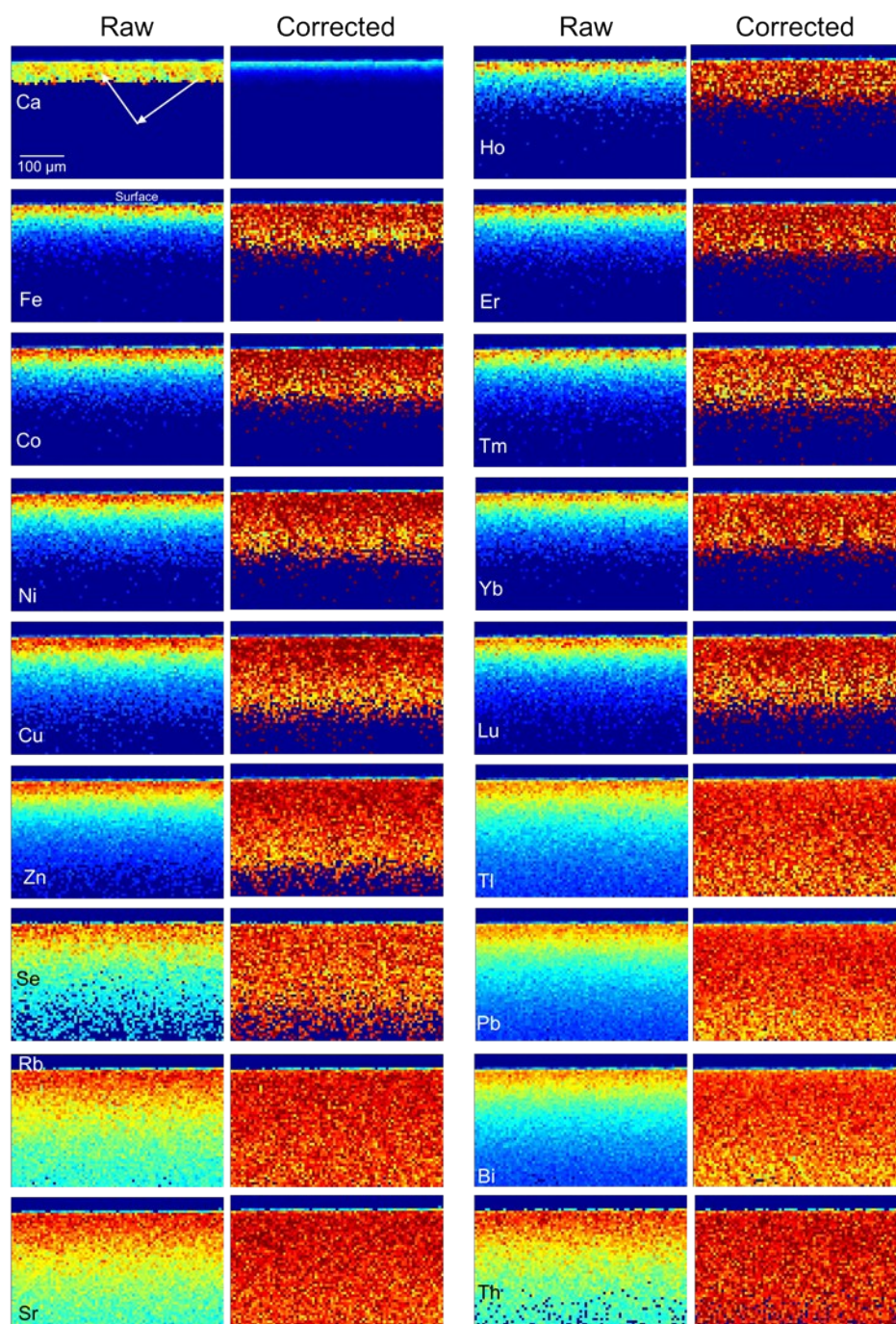


Figure S4. The raw and corrected data X-ray fluorescence of Ca, Fe, Co, Ni, Cu, Zn, Se, Rb, Sr, Ho, Er, Tm, Yb, Lu, Ti, Pb, Bi, and Th from the middle of SRM 611 (glass with trace elements). Because intensities of low-atomic number elements cannot be collected after certain depth due to self absorption, the mass distribution of elements with atomic number  $<30$  was assumed the same as Th for correction purpose. The top of the imaging area is the surface. The maps were plotted at the same intensity scale for the raw and corrected data for each element. The map size is  $250 \times 400 \mu\text{m}$ .

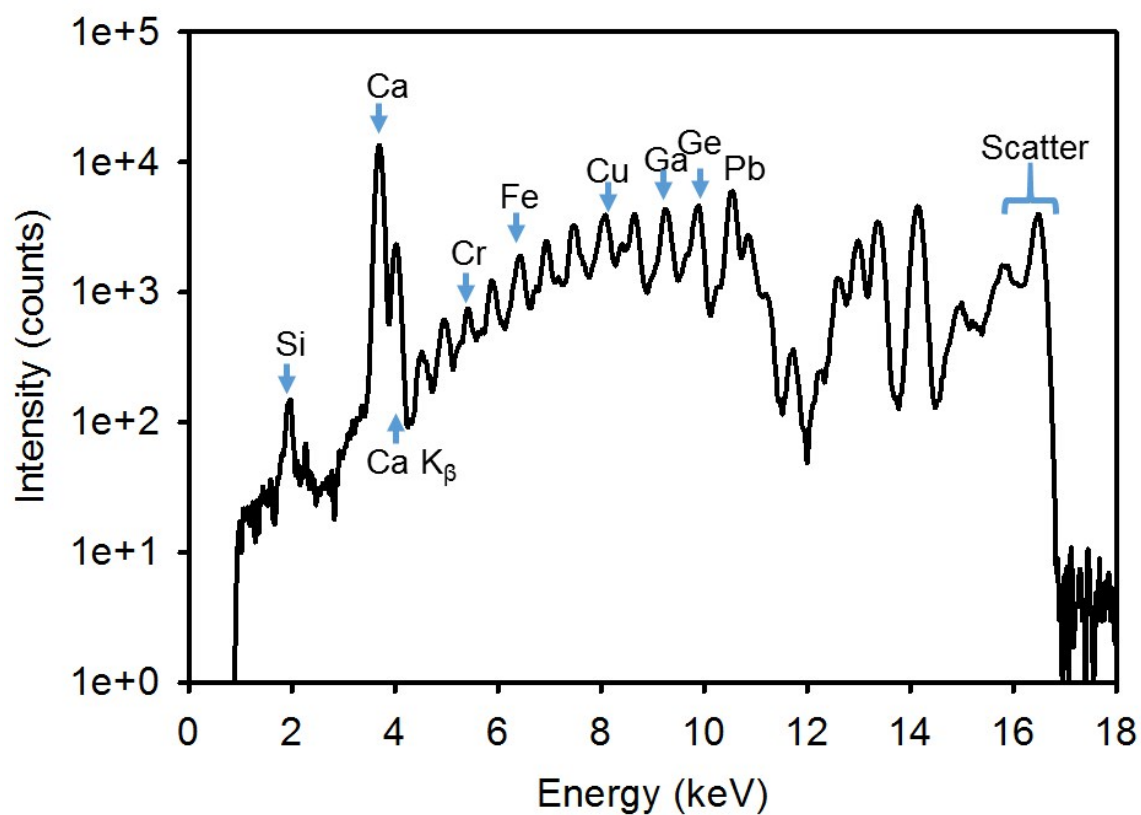


Figure S5. XRF spectrum collected from the surface area of SRM 611 in Fig. S4 (in the middle of the reference material). The peaks indicated by element name represent the  $K_{\alpha}$  line. The  $K_{\beta}$  line of Ca and scatter are also labeled. The incident energy was 16.5 keV.

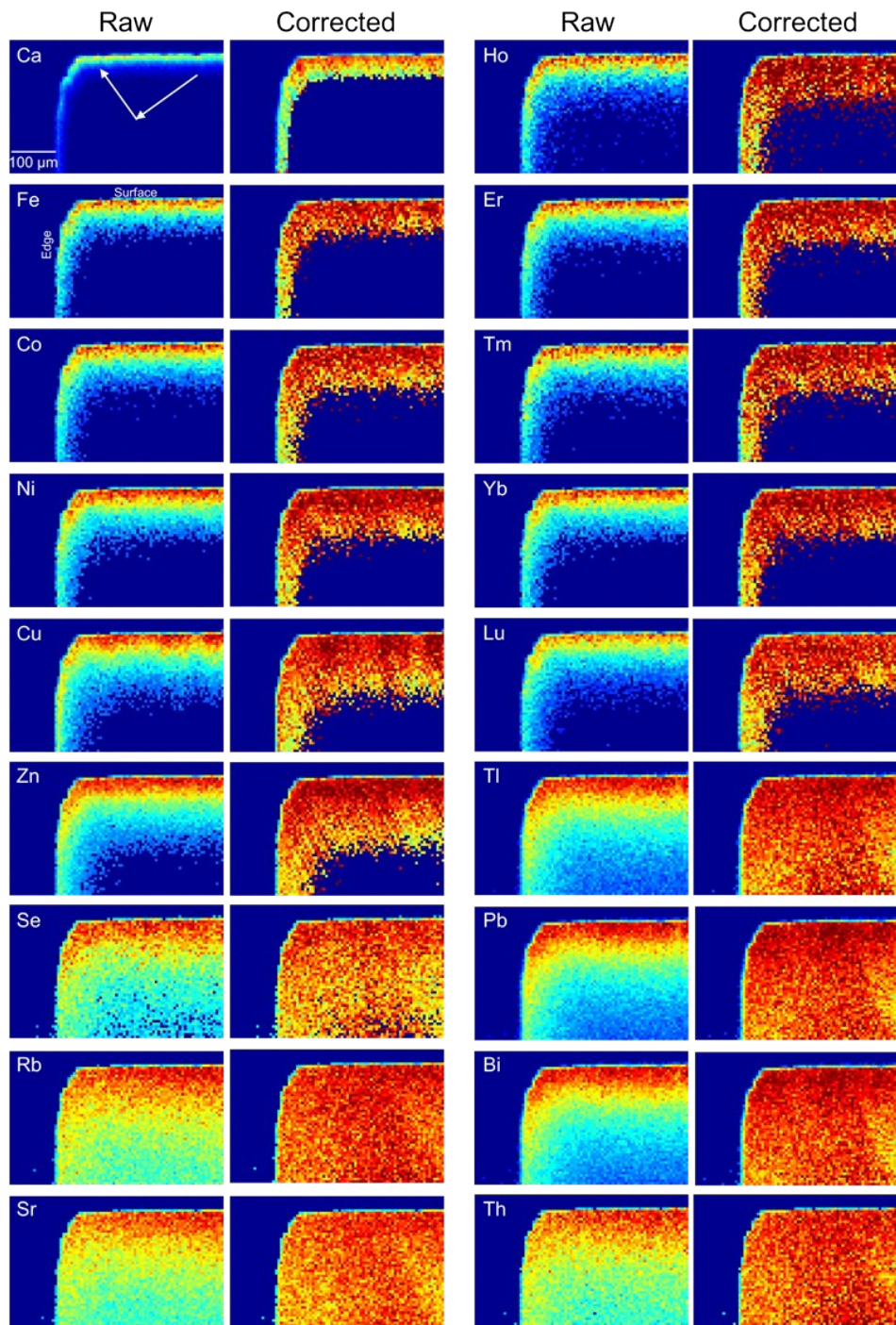


Figure S6. The raw and corrected data X-ray fluorescence of Ca, Fe, Co, Ni, Cu, Zn, Se, Rb, Sr, Ho, Er, Tm, Yb, Lu, Ti, Pb, Bi, and Th from the edge of SRM 611 (glass with trace elements). Because intensities of low-atomic number elements cannot be collected after certain depth due to self absorption, the mass distribution of elements with atomic number  $<30$  was assumed the same as Th for correction purpose. The maps were plotted at the same intensity scale for the raw and corrected data for each element. The map size is  $250 \times 400 \mu\text{m}$ .

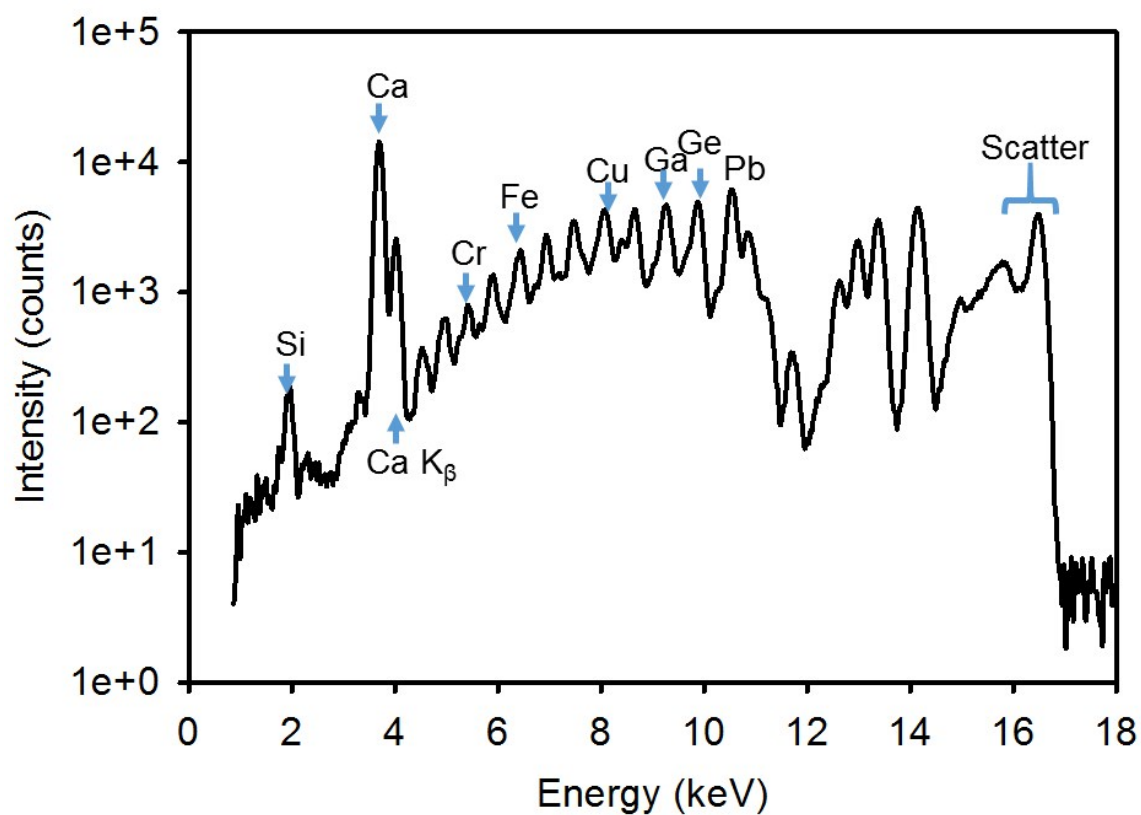


Figure S7. XRF spectrum collected from the surface area of SRM 611 in Fig. S6. The peaks indicated by element name represent the  $K_{\alpha}$  line. The  $K_{\beta}$  line of Ca and scatter are also labeled. The incident energy was 16.5 keV.

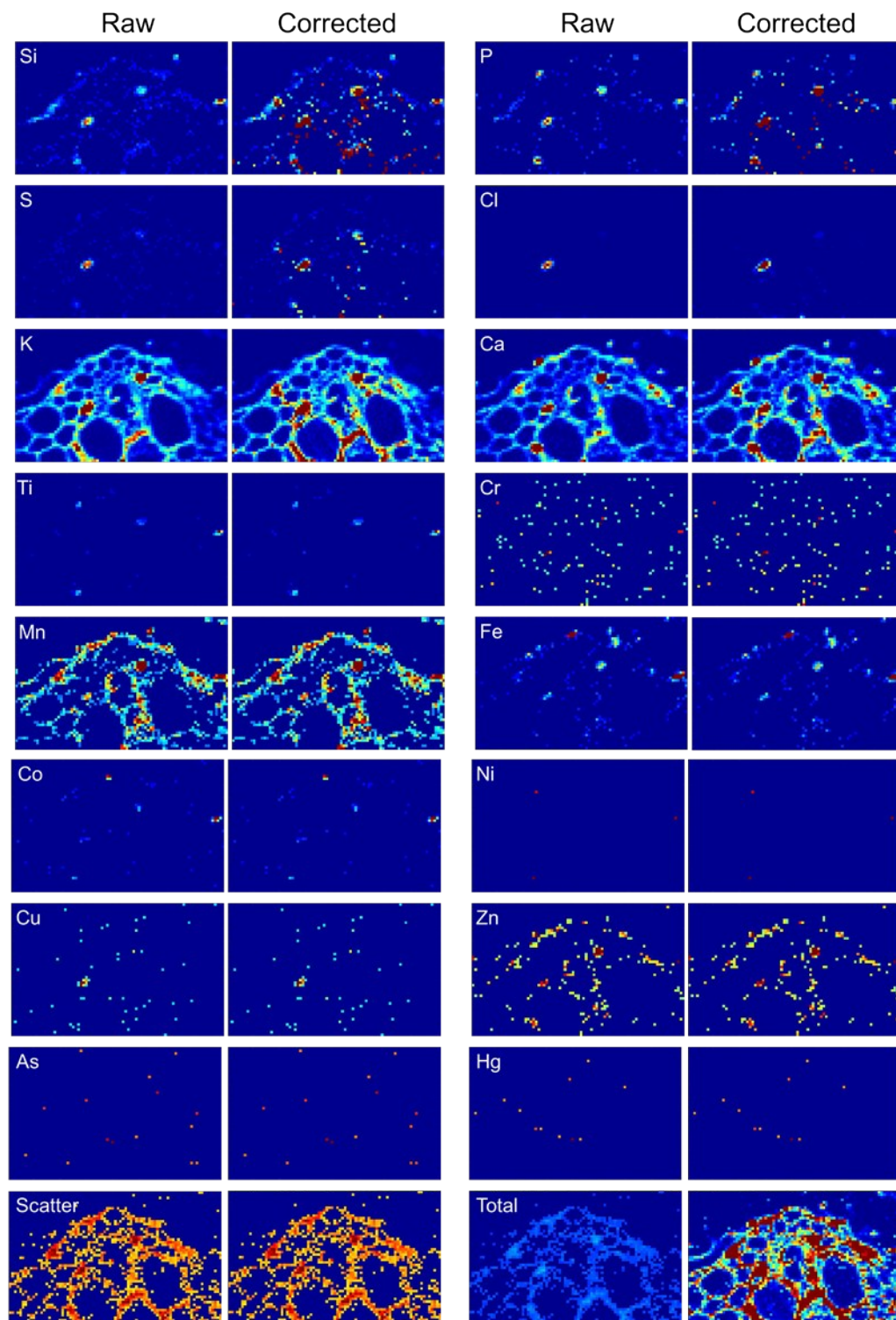


Figure S8. The raw and corrected data X-ray fluorescence of selected elements from a fresh switchgrass biochar particle. The top of the imaging area is the surface of the particle. The maps were plotted at the same intensity scale for the raw and corrected data for each element. The imaging area is 250×400  $\mu\text{m}$ .

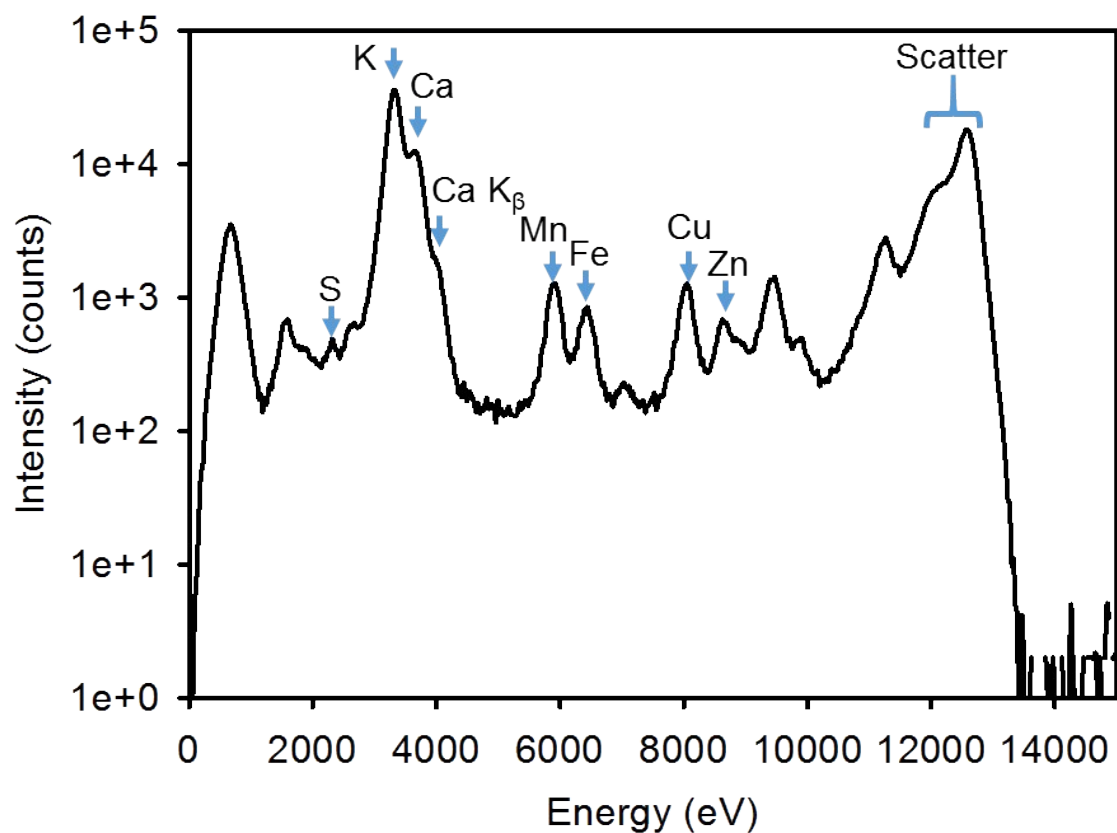
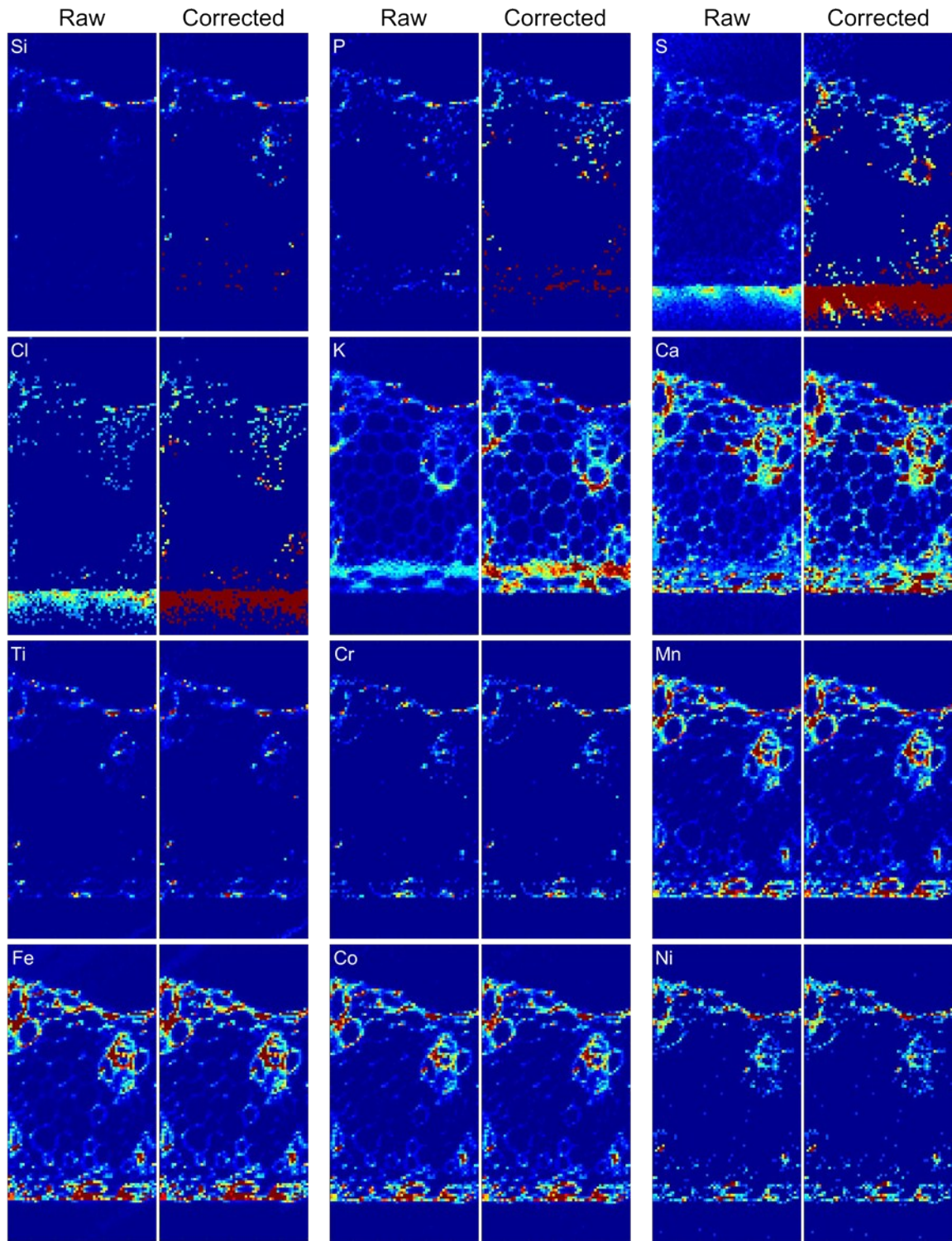


Figure S9. XRF spectrum collected from the surface area of the fresh biochar particle in Fig. S8. The peaks indicated by element name represent the  $K_{\alpha}$  line. The  $K_{\beta}$  line of Ca and scatter are also labeled in both spectra, and the  $L_{\alpha}$  line of Hg is labeled. The incident energy was 12.6 keV.



Continued

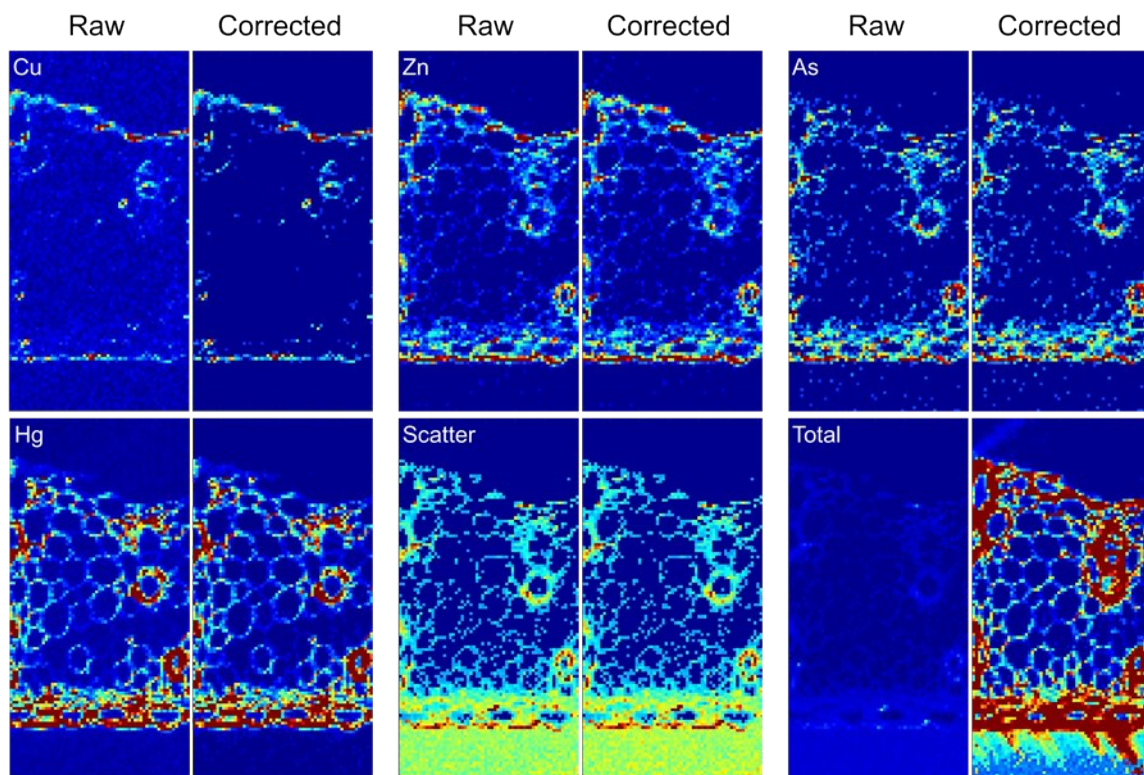


Figure S10. The raw and corrected data X-ray fluorescence of selected elements from an aged switchgrass biochar particle. The top of the imaging area is the surface of the particle. The maps were plotted at the same intensity scale for the raw and corrected data for each element. The imaging area is  $600 \times 300 \mu\text{m}$ .

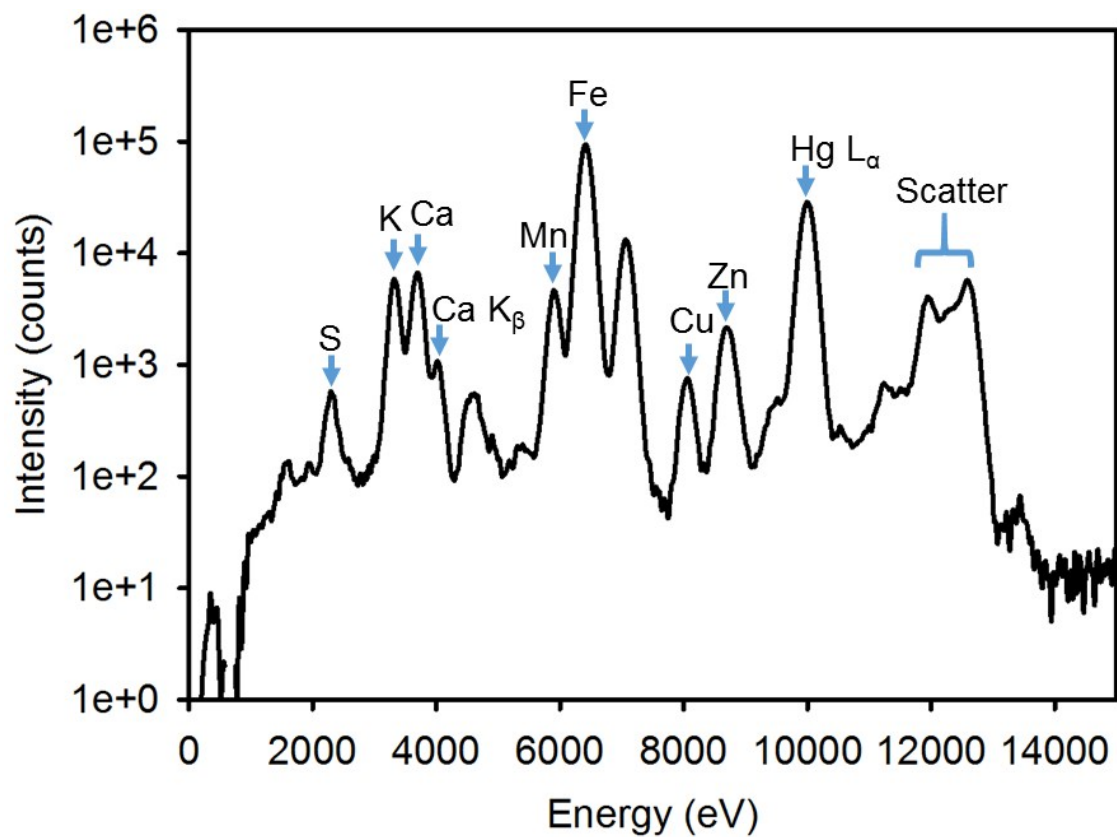


Figure S11. XRF spectra collected from the surface area of the aged biochar particle in Fig. S10. The peaks indicated by element name represent the  $K_{\alpha}$  line. The  $K_{\beta}$  line of Ca and scatter are also labeled in both spectra, and the  $L_{\alpha}$  line of Hg is labeled. The incident energy was 12.6 keV.

## References

- (1) NIST SRM 1834 Certificate. **1990**.
- (2) Hollocher, K.; Ruiz, J. *Geostandard. Newslett.* **1995**, *19*, 27-34.
- (3) NIST SRM 611 Certificate. **2017**.
- (4) Pearce, N. J. G.; Perkins, W. T.; Westgate, J. A.; Gorton, M. P.; Jackson, S. E.; Neal, C. R.; Chenery, S. P. *Geostandard. Newslett.* **1997**, *21*, 115-144.
- (5) Hinton, R. W. *Geostandard. Newslett.* **1999**, *23*, 197-207.
- (6) Liu, P.; Ptacek, C. J.; Blowes, D. W.; Berti, W. R.; Landis, R. C. *J. Environ. Qual.* **2015**, *44*, 684-695.
- (7) Liu, P.; Ptacek, C. J.; Blowes, D. W.; Landis, R. C. *J. Hazard. Mater.* **2016**, *308*, 233-242.
- (8) Liu, P.; Ptacek, C. J.; Blowes, D. W.; Finfrock, Y. Z.; Gordon, R. A. *J. Hazard. Mater.* **2017**, *325*, 120-128.
- (9) Sadaka, S.; Sharara, M. A.; Ashworth, A.; Keyser, P.; Allen, F.; Wright, A. *Energies* **2014**, *7*, 548-567.
- (10) Cherney, J. H.; Paddock, K. M. Harvest management and switchgrass composition. Bioenergy Information Sheet #11. <http://forages.org/index.php/grass-biofuels/resources/information-sheets> (Accessed by October 2016)
- (11) El Bassam, N. *Handbook of Bioenergy Crops: A Complete Reference to Species, Development and Applications*; Earthscan: New York, 2010.
- (12) Smolek, S.; Nakazawa, T.; Tabe, A.; Nakano, K.; Tsuji, K.; Strelci, C.; Wobrauschek, P. *X Ray Spectrom.* **2014**, *43*, 93-101.